Magnetic Resonance Imaging 31 (2013) 789–795

Contents lists available at SciVerse ScienceDirect

Magnetic Resonance Imaging

journal homepage: www.mrijournal.com

Improved dynamic MRI reconstruction by exploiting sparsity and rank-deficiency

Angshul Majumdar

Indraprastha Institute of Information Technology, Delhi

ARTICLE INFO

Article history:
Received 6 September 2012
Revised 17 October 2012
Accepted 30 October 2012

Keywords:
Dynamic MRI
Compressed Sensing

ABSTRACT

In this paper we address the problem of dynamic MRI reconstruction from partially sampled K-space data. Our work is motivated by previous studies in this area that proposed exploiting the spatiotemporal correlation of the dynamic MRI sequence by posing the reconstruction problem as a least squares minimization regularized by sparsity and low-rank penalties. Ideally the sparsity and low-rank penalties should be represented by the l_0-norm and the rank of a matrix; however both are NP hard penalties. The previous studies used the convex l_1-norm as a surrogate for the l_0-norm and the non-convex Schatten-q norm ($0<q\leq 1$) as a surrogate for the rank of matrix. Following past research in sparse recovery, we know that non-convex l_p-norm ($0<p\leq 1$) is a better substitute for the NP hard l_0-norm than the convex l_1-norm. Motivated by these studies, we propose improvements over the previous studies by replacing the l_1-norm sparsity penalty by the l_p-norm. Thus, we reconstruct the dynamic MRI sequence by solving a least squares minimization problem regularized by l_p-norm as the sparsity penalty and Schatten-q norm as the low-rank penalty. There are no efficient algorithms to solve the said problems. In this paper, we derive efficient algorithms to solve them. The experiments have been carried out on Dynamic Contrast Enhanced (DCE) MRI datasets. Both quantitative and qualitative analysis indicates the superiority of our proposed improvement over the existing methods.

1. Introduction

In this work we address the problem of reconstructing dynamic Magnetic Resonance Imaging (MRI) sequences from under-sampled K-space data of each frame. The reconstruction is carried out offline, i.e., posthumously after all the data (K-space samples from all frames) have been collected. Such a reconstruction is typically formulated as an under-determined linear inverse problem. Since it is under-determined, additional assumptions regarding the structure of the dynamic MRI sequence is required in order to obtain a physically viable solution.

Each frame of the dynamic MRI sequence is spatially correlated (locally). This is a well known fact which has been used for reconstructing static Magnetic Resonance (MR) images [1,2]. Also since the frames are acquired after short intervals of time, they are temporally correlated. Recent studies in dynamic MRI reconstruction [3–14] exploit this spatiotemporal correlation while reconstructing them from under-sampled K-space data.

The dynamic MRI data acquisition model can be expressed as follows:

$$y_t = RFx_t + \eta_t \tag{1}$$

where X_t denotes the MR image frame at the t^{th} instant, T is the total number of frames collected, y_t is the collected K-space data for the t^{th} frame, F is the Fourier operator (2D or 3D as the case may be) which maps the image space to the K-space, R is the under-sampling mask on the K-space, x_t is the vectorized MR image formed by row/column concatenation of the image matrix X_t and η_t is the system noise assumed to be Normally distributed with variance σ^2.

The problem is to recover all X_t's ($t=1...T$) from the given the collected K-space data y_t's for all the frames.

The motivation behind this work is straightforward. The aim is to acquire a dynamic MRI sequence with high spatial and temporal resolution. However as the speed of data acquisition is limited there is always a trade-off between spatial and temporal resolution. Conventional methods require the full K-space to be sampled on a uniform Cartesian grid from which the frames are reconstruction via inverse Fast Fourier Transform (FFT). In such a circumstance, in order to get high temporal resolution, the spatial resolution needs to be sacrificed. Recent developments in dynamic MRI reconstruction [3–14] showed that full sampling of the K-space is not required; one can partially sample the K-space for each frame and employ a smart reconstruction algorithm that exploits the spatiotemporal correlation of the sequence in order to reconstruct it. This allows for improvement in temporal resolution without sacrificing the spatial resolution. An example will make it clear: suppose by traditional means one can acquire dynamic MRI sequences of size 256 × 256 pixels at the rate of one frame per second. If the frame rate is required to be increased 4 fold, conventional methods would require reducing the spatial resolution to 128 × 128 pixels. However, recent studies show that instead of reducing the spatial resolution, one can reduce the sampling requirement for each frame by 4 fold (by collecting 25% of the K-space samples from each frame) and thereby

E-mail address: angshul@iiitd.ac.in.

0730-725X/$ – see front matter © 2013 Elsevier Inc. All rights reserved.
http://dx.doi.org/10.1016/j.mri.2012.10.026

increase the frame rate by 4 times. Thus temporal resolution is increased without sacrificing spatial resolution (there is a slight deterioration in image quality owing to under-sampling of the K-space).

The first studies that reconstructed dynamic MRI sequences from under-sampled K-space data exploited the sparsity of the image sequence in a transform domain in order to reconstruct it [3–9]. Later on, it was argued that since the frames are correlated with each other, the whole sequence (when expressed as a matrix whose columns are the frames in vector form) can be expressed in terms of very few temporal basis functions. Under this assumption the sequence can be modeled as a low-rank matrix. This assumption was used in [10,11] to reconstruct the dynamic MRI sequence. The most recent works in this area combine transform domain sparsity with low-rank property to reconstruct the sequence [12–14]. These studies [12–14] have shown to yield better reconstruction results compared to the previous ones [3–11].

Following previous work [12–14] we model the dynamic MRI sequence as a matrix which is simultaneously sparse (in a transform domain) and also has a low-rank. The novelty of our work lies in the mathematical formulation of the reconstruction problem. We propose the reconstruction as a least squares optimization problem which is regularized by the non-convex l_p-norm ($0<p\le 1$) as the sparsity penalty and the non-convex Schatten-q norm ($0<q\le 1$) as the low-rank penalty. It differs from the previous studies [12–14] in the choice for sparsity penalty; they used a convex l_1-norm as the sparsity penalty where as we have used a non-convex l_p-norm. The proposed change in the sparsity penalty leads to significant improvements in the reconstruction results.

Understanding the differences between our proposed method and the existing ones is easier when the background literature in dynamic MRI reconstruction from under-sampled K-space data is known. We will briefly review the literature in this area in the following section. Our proposed method is discussed in section 3. Our proposed formulation requires solving certain optimization problems which have not been encountered before and therefore there exists no efficient algorithms to solve them. In section 4, we derive the algorithms to solve the required optimization problems. The experimental results will be shown in section 5. The conclusions of this work are discussed in Section 6.

2. Literature review

The data acquisition model for dynamic MRI (1) can be expressed as,

$$Y = RFX + \eta \tag{2}$$

where $Y=[y_1|\ldots|y_T]$, $X=[x_1|\ldots|x_T]$, $\eta=[\eta_1=\eta_1|\ldots|\eta_T]$, and T is the total number of frames.

The problem is to recover the dynamic MRI sequence X given the K-space samples Y. Since, the K-space is partially sampled the problem (2) is under-determined and therefore does not have a unique solution. As we mentioned before, to get a physically viable solution to (2), one needs to have a prior knowledge about X.

In a dynamic MRI sequence the difference between frames arises from motion (heart beat) or from changes in concentration (cardiac perfusion). The motion/concentration change is typically concentrated only in certain areas of the cross section under study. Thus along the temporal direction of the sequence, (along rows of X), only certain areas (corresponding to motion/change in concentration) have major variations in pixel values while the rest of the areas have negligible variation. Also the frame images are spatially correlated (locally).

Under such an assumption on the dynamic MRI sequence, the signal X will be approximately sparse under several transforms –

1. When the 1D Fourier transform is applied along the temporal direction, the resultant signal in the x-f[1] space will be approximately sparse since most areas show small variation in pixel values and will lead to Fourier transform coefficients near to zero; only the small areas where the variation is high will result in high valued coefficients. Several studies have used this information to reconstruct the dynamic MRI sequence [5–7]. Mathematically the reconstruction problem is formulated as follows:

$$\min_x \|I\otimes F_{1D}(x)\|_1 \text{ subject to } \|Y-RFX\|_F^2\le\varepsilon \tag{3}$$

where $\|.\|_F$ is the Frobenius norm of the matrix, $\|.\|_1$ is the l_1-norm of the vector, x is the vectorized forms of X, F_{1D} is the 1D Fourier transform and $\varepsilon=TN\sigma^2$ assuming that each frame has N pixels.

Here $I\otimes F_{1D}$ is the Kronecker product.[2] In the original studies the Kronecker product formulation is not used; we introduce it here to make the notation more compact. The l_1-norm imposes the sparsity penalty.

2. When temporal differencing is applied on X, the resultant difference signal is also approximately sparse since most of the areas with low time variations cancel each other (leading to zeroes after differencing) while only small areas showing motion/change in concentration correspond to high values in the resulting difference signal. The reconstruction problem formulated in this work [8] can be expressed as follows:

$$\min_x TV_t(x) \text{ subject to } \|Y-RFX\|_F^2\le\varepsilon \tag{4}$$

where $TV_t=\sum_{i=1}^{N^2}\|\nabla_t x_i\|$ and ∇_t denotes the temporal differentiation for the i^{th} pixel.

In essence, the approach in [8] differs only slightly from [5–7]. In [5–7] it is assumed that the signal varies smoothly over time, so that it is sparse in the temporal Fourier transform. In [8], temporal Fourier transform is not applied, but the signal is assumed to be smoothly varying with time with only a finite number of discontinuities, so that it will be sparse in the temporal differencing domain.

3. In [5–7] and [8] only the temporal correlation is used. The fact that each of the frames in the dynamic MRI sequence is spatially correlated is not utilized. When spatio-temporal correlation of the dynamic MRI sequence is exploited the resulting reconstruction is even more accurate. In [3,4] the spatial correlation within each frame is captured by the wavelet transform (W) and the temporal correlation is captured by the 1D Fourier transform. These works reconstructed the dynamic MRI sequence by solving a problem of the following form:

$$\min_x \|W\otimes F_{1D}(x)\|_1 \text{ subject to } \|Y-RFX\|_F^2\le\varepsilon \tag{5}$$

4. Instead of such transforms, the spatio-temporal differencing can also be used to capture the spatio-temporal redundancy in the dynamic MRI sequence. This leads to the following optimization problem [9]:

$$\min_x \|\nabla_s\otimes\nabla_t(x)\|_1 \text{ subject to } \|Y-RFX\|_F^2\le\varepsilon \tag{6}$$

[1] The signal X is said to be in the x-t space, where x refers to spatial domain and t refers to temporal direction. When 1D Fourier transform is applied on X in the temporal direction, the resultant signal is in the x-f space where f refers to temporal frequency.

[2] Let $A_{m\times n}$ and $B_{p\times q}$ be two matrices and $A=\begin{bmatrix} a_{11} & \ldots & a_{1n} \\ \ldots & \ldots & \ldots \\ a_{m1} & \ldots & a_{mn}\end{bmatrix}$, then $A\otimes B=\begin{bmatrix} a_{11}B & \ldots & a_{1n}B \\ \ldots & \ldots & \ldots \\ a_{m1}B & \ldots & a_{mn}B\end{bmatrix}$.

where ∇_s is the finite differencing operator in the spatial domain and ∇_t is the temporal differencing operator.

There are a few papers [10,11] that assume the signal X to be rank deficient. Since the columns of X (i.e. image frames) are correlated, the signal X can be expressed by very few temporal basis functions and hence it is approximately rank deficient. Based on this assumption, the matrix X can be recovered by solving the following,

$$\min_X \|X\|_* \text{subject to } \|Y-RFX\|_F^2 \leq \varepsilon \tag{7}$$

However in the original work [10,11] the Nuclear Norm was not used as the objective function for promoting rank deficiency. They used a power factorization based method instead.

A recent method called '*k-t* SLR' [12,13] proposes minimization of a combination of rank-deficiency of the signal in the *x-t* space and its sparsity in Spatio-Temporal differencing domain. The following optimization problem is proposed,

$$\min_X \|Y-RFX\|_F^2 + \lambda_1 \|\nabla_s \otimes \nabla_t(x)\|_1 + \lambda_2 \|X\|_{S_q}^q \tag{8}$$

Here $\|Y-RFX\|_F^2$ is the data fidelity term, $\|\nabla_s \otimes \nabla_t(X)\|_1$ is the convex sparsity penalty and the non-convex Schatten-q norm $\|X\|_{S_q}^q$ is the penalty on rank-deficiency. The constants λ_1 and λ_2 control the relative importance of the sparsity and rank-deficiency penalties. The k-t SLR method yields better results than other reconstruction techniques; this is because they combine sparsity with the low-rank property instead of using only one of them.

Following the success of k-t SLR, a recent work proposed a variation [14]. The fundamental idea remains the same (combining sparsity with rank-deficiency) but it differs from k-t SLR in two aspects –

1. Instead of assuming the signal to be sparse in the spatio-temporal differencing domain, it was assumed to be sparse in the *x-f* space.
2. Instead of using Schatten-q norm as the penalty on rank-deficiency, a power factorization based method was used to account for the low-rank property.

3. Proposed approach

Our work follows from k-t SLR [12,13] and the method proposed in [14]. The basic assumption is the same, i.e. the signal X is simultaneously sparse (in a transform domain) and low-rank. We propose an improvement over the previous studies. Before explaining the improvement, we will have a closer look at the reconstruction problems. The k-t SLR [12,13] assumes that the signal is sparse under spatio-temporal differencing and requires solving the following problem:

$$\min_X \|Y-RFX\|_F^2 + \lambda_1 \|\nabla_s \otimes \nabla_t(x)\|_1 + \lambda_2 \|X\|_{S_q}^q \tag{9}$$

The other study [14] assumes that the signal is sparse in the *x-f* space and therefore requires solving a problem of the following form:

$$\min_X \|Y-RFX\|_F^2 + \lambda_1 \|I \otimes F_{1D}(x)\|_1 + \lambda_2 \|X\|_{S_q}^q \tag{10}$$

In Eqs. (9) and (10), the l_1-norm imposes the sparsity penalty and the Schatten-q norm imposes the low-rank penalty. Strictly speaking, the original study [14] did not employ a Schatten-q norm but used a power factorization based method instead. The power factorization based method is non-convex and approximately solves the Schatten-q norm minimization problem.

The idea of using the l_1-norm for sparse recovery follows from Compressed Sensing [15,16]. Ideally the sparsity penalty should be the l_0-norm; however solving the l_0-norm minimization problem is NP hard. The l_1-norm is the nearest convex envelope for the l_0-norm; theoretical studies in Compressed Sensing have shown that the convex l_1-norm will be a good substitute for the NP hard l_0-norm for a wide range of problems. Owing to the convexity, problems involving l_1-norms are is easy to be analysed and implemented. However studies in non-convex Compressed Sensing [17–19] showed that if instead of the convex l_1-norm, a non-convex l_p-norm ($0<p\leq 1$) is used, then better recovery results can be guaranteed. This is because the non-convex l_p-norm is a closer surrogate to the NP hard l_0-norm than the convex l_1-norm. The theoretical results in l_p -norm minimization prompted researchers in MRI reconstruction to experiment with such non-convex penalties [2,20,21]. They found that, better reconstruction results can be indeed be obtained by replacing the convex l_1-norm by the non-convex l_p-norm.

Following the success of non-convex l_p-norm over convex l_1-norm in sparse recovery problems of static MRI, we propose to replace the convex l_1-norms in (9) and (10) by their non-convex counterparts (l_p-norm). In this work, we propose to recover the dynamic MRI sequence by solving the following optimization problems:

$$\min_X \|Y-RFX\|_F^2 + \lambda_1 \|\nabla_s \otimes \nabla_t(x)\|_p^p + \lambda_2 \|X\|_{S_q}^q \tag{11}$$

$$\min_X \|Y-RFX\|_F^2 + \lambda_1 \|I \otimes F_{1D}(x)\|_p^p + \lambda_2 \|X\|_{S_q}^q \tag{12}$$

Here (11) and (12) are counterparts of [12,13] and [14] respectively but with l_1-norms replaced by l_p-norms. There is a simpler formulation to (12). The *x-f* space $I \otimes F_{1D}(x)$ can also be expressed as $F_{1D}X^T$. Therefore, (12) can be alternately expressed as:

$$\min_X \|Y-RFX\|_F^2 + \lambda_1 \left\|F_{1D}X^T\right\|_p^p + \lambda_2 \left\|X^T\right\|_{S_q}^q \tag{13}$$

We replace the Schatten-q norm in (13) by its equivalent Ky-Fan norm ($\|U\|_{S_q}^q = Tr\left(U^TU\right)^{q/2}$) and substitute $Z=F_{1D}X^T$. Using these substitutions (13) takes the following form:

$$\min_Z \|Y-RFZF_{1D}\|_F^2 + \lambda_1 \|Z\|_p^p + \lambda_2 Tr\left(Z^TZ\right)^{q/2} \tag{14}$$

Since $\|F_{1D}^TZ\|_{S_q}^q = Tr(Z^TF_{1D}F_{1D}^TZ)^{q/2} = Tr(Z^TZ)^{q/2}$ because F_{1D} is an orthogonal transform.

Using the Kronecker product notation, the term $\|Y-RFZF_{1D}\|_F^2$ in (14) can be expressed as, $\|y-F_{1D}^T \otimes RFz\|_2^2$ where $z=vec(Z)$ and $y=vec(Y)$, i.e. the operator 'vec' converts a matrix to a vector by row/column concatenation.

Using these substitutions, we obtain the simplified version of (12):

$$\min_z \left\|y - F_{1D}^T \otimes RFz\right\|_2^2 + \lambda_1 \|z\|_p^p + \lambda_2 Tr\left(Z^TZ\right)^{q/2} \tag{15}$$

It is not possible to simplify (11) owing to the non-separability of the differencing operation. But the Schatten-q norm in (11) can be replaced by its equivalent Ky-Fan norm leading to the following:

$$\min_X \|Y-RFX\|_F^2 + \lambda_1 \|\nabla_s \otimes \nabla_t(x)\|_p^p + \lambda_2 Tr\left(X^TX\right)^{q/2} \tag{16}$$

The problem (15) turns out to be a synthesis prior problem, whereas (16) is an analysis prior problem [22]. The terms synthesis and analysis priors only apply to the sparsity penalties. Unfortunately there are no algorithms to solve either (15) or (16); thus we need to derive them. In the following section, we derive efficient algorithms to solve these.

4. Optimization algorithms

In this section we derive algorithms to solve (15) and (16). The derivation is based on the Majorization Minimization approach [22]. The generic MM algorithm is as follows:

Let $J(x)$ be the (scalar) function to be minimized

1. Set iteration count $k=0$ and initialize x_0.
   a. Repeat step 2-4 until a suitable stopping criterion is met.
2. Choose $G_k(x)$ such that
   a. $G_k(x) \geq J(x)$ for all x.
   b. $G_k(x_k)=J(x_k)$.
3. Set x_{k+1} as the minimizer for $G_k(x)$.
4. Set $k=k+1$, go to step 2.

4.1. Solving the synthesis prior problem

For our problem the function to be minimized is

$$J(x) = \|y-Ax\|_2^2 + \lambda_1 \|x\|_p^p + \lambda_2 Tr\left(X^T X\right)^{q/2}$$

Here $A=F_{1D}^T \otimes RF$ and $X=Z$. These substitutions are made to make the notations simpler.

There is no closed form solution to $J(x)$, it must be solved iteratively. At each iteration we choose,

$$G_k(x) = ||y-Ax||_2^2 + (x-x_k)^t\left(aI-A^T A\right)(x-x_k) + \lambda_1 \|x\|_p^p + \lambda_2 Tr\left(X^T X\right)^{q/2} \tag{17}$$

$G_k(x)$ satisfies the condition for MM algorithm when $a \geq \max\ eigvalue(A^T A)$.

Now $G_k(x)$ can be alternately expressed as follows,

$$G_k(x) = a\left\|x_k + \frac{1}{a}A^T(y-Ax) - x\right\|_2^2 + \lambda_1 \|x\|_p^p + \lambda_2 Tr\left(X^T X\right)^{q/2} + K \tag{18}$$

where K consists of terms independent of x.

Minimizing (18) is the same as minimizing the following,

$$G_k^{'}(x) = \|b-x\|_2^2 + \frac{\lambda_1}{a}\|x\|_p^p + \frac{\lambda_2}{a} Tr\left(X^T X\right)^{q/2} \tag{19}$$

where $b = x_k + \frac{1}{a}A^T(y-Ax_k)$.

To minimize (19) we take its derivative,

$$\nabla G_k^{'}(x) = 2x - 2b + \frac{\lambda_1}{a} p|x|^{p-2} \cdot x + \frac{\lambda_2}{2a} q\left(XX^T\right)^{\frac{q}{2}-1} X \tag{20}$$

where '.' denotes element wise product.

Setting the gradient to zero, one gets,

$$(I+D)x = b \tag{21}$$

where $D = \frac{\lambda_1}{2a} pDiag\left(|x|^{p-2}\right) + \frac{\lambda_2}{4a} qI \otimes \left(XX^T\right)^{\frac{q}{2}-1}$.

Here the Diag operator creates a diagonal matrix out of the vector $|x|^{p-2}$.

The problem (21) represents a system of linear equations. It should be noted that the system $(I+D)$ is symmetric. Hence it can be efficiently solved by newly developed MINRES-QLP algorithm [23].

Based on this derivation, we propose the following algorithm to solve (15).

Intitialize: $x_0 = 0$
Repeat until: $\|y-Ax\|_2^2 \leq \varepsilon$
Step 1. $b = x_k + \frac{1}{a}A^T(y-Ax_k)$
Step 2. $D = \frac{\lambda_1}{2a} pDiag\left(|x_{k-1}|^{p-2}\right) + \frac{\lambda_2}{4a} qI \otimes \left(X_{k-1}X_{k-1}^T\right)^{\frac{q}{2}-1}$
Step 3. Compute x by solving $(I+D)x = b$
End

4.2. Solving the analysis prior problem

The task is to solve Eq. (16). For ease of representation, we express it in the following form:

$$\min_X \|Y-AX\|_F^2 + \lambda_1 \|Hx\|_p^p + \lambda_2 Tr\left(X^T X\right)^{q/2} \tag{22}$$

where $A=RF$ and $H=\nabla_s \otimes \nabla_t$.

The function to be minimized is the following:

$$J(X) = \|Y-AX\|_F^2 + \lambda_1 \|Hx\|_p^p + \lambda_2 Tr\left(X^T X\right)^{q/2} \tag{23}$$

Following the Majorization Minimization approach at each iteration we choose,

$$G_k(x) = \|Y-AX\|_F^2 + (x-x_k)^t\left(aI-A^T A\right)(X-X_k) + \lambda_1 \|Hx\|_p^p + \lambda_2 Tr\left(X^T X\right)^{q/2} \tag{24}$$

$G_k(x)$ satisfies the condition for MM algorithm when $a \geq \max\ eigvalue(A^T A)$

Now $G_k(x)$ can be alternately expressed as follows,

$$G_k(x) = a\left\|X_k + \frac{1}{a}A^T(Y-AX) - X\right\|_2^2 + \lambda_1 \|Hx\|_p^p + \lambda_2 Tr\left(X^T X\right)^{q/2} + K \tag{25}$$

where K consists of terms independent of x.

Minimizing (25) is the same as minimizing the following,

$$G_k^{'}(x) = \|B-X\|_2^2 + \frac{\lambda_1}{a}\|Hx\|_p^p + \frac{\lambda_2}{a} Tr\left(X^T X\right)^{q/2} \tag{26}$$

where $B = X_k + \frac{1}{a}A^T(Y-AX_k)$.

To minimize (26), we take its derivative,

$$\nabla G_k^{'}(x) = 2X - 2B + \frac{\lambda_1}{a} H^T \Omega Hx + \frac{\lambda_2}{2a} q\left(XX^T\right)^{\frac{q}{2}-1} X, \quad \text{where } \Omega = diag\left(p|Hx|^{p-2}\right) \tag{27}$$

Setting the gradient to zero, one gets

$$\left(I + \frac{\lambda_1}{2a} H^T \Omega H + \frac{\lambda_2}{4a} qI \otimes \left(XX^T\right)^{\frac{q}{2}-1}\right)x = b, \text{where } b = vec(B) \tag{28}$$

Since Eq. (28) is not separable like Eq. (20), finding the solution for the analysis prior problem is slightly more involved than the synthesis prior one. We express Eq. (28) as follows:

$$\left(M + \frac{\lambda_1}{2a} H^T \Omega H\right)x = b, \text{where } M = I + \frac{\lambda_2}{4a} qI \otimes \left(XX^T\right)^{\frac{q}{2}-1} \tag{29}$$

Using the matrix inversion lemma,

$$\left(M+\frac{\lambda_1}{2a}H^T\Omega H\right)^{-1} = M^{-1}-M^{-1}H^T\left(\frac{2a}{\lambda_1}\Omega^{-1}+HM^{-1}H^T\right)^{-1}HM^{-1}$$

Therefore we have the following identity,

$$x=M^{-1}b-M^{-1}H^T\left(\frac{2a}{\lambda_1}\Omega^{-1}+HM^{-1}H^T\right)^{-1}HM^{-1}b \tag{30}$$

Or equivalently,

$$z=\left(\frac{2a}{\lambda_1}\Omega^{-1}+HM^{-1}H^T\right)^{-1}HM^{-1}b \tag{31}$$

$$x=M^{-1}b-M^{-1}H^Tz \tag{32}$$

Solving z requires solving the following,

$$\tilde{z}=\left(\frac{2a}{\lambda_1}\Omega^{-1}+HM^{-1}H^T\right)^{-1}HM^{-1/2}b,\, z=M^{-1/2}\tilde{z} \tag{33}$$

Here $M^{-1/2}$ is the Cholesky decomposition of M. The decomposition exists since M is symmetric positive definite (follows from the definition of M in (29)).

It is possible to solve $\tilde{z}$ by Conjugate Gradient method [24]. Once $\tilde{z}$ is solved, finding the value of x is straightforward.

This derivation leads to the following iterative algorithm:

Intitialize: $x_0=0$
Repeat until: $\|y-Ax\|_2^2\le\varepsilon$
Step 1. $B=X_k+\frac{1}{a}A^T(Y-AX_k)$
Step 2. $M=I+\frac{\lambda_2}{4a}qI\otimes(XX^T)^{\frac{q}{2}-1},\, b=vec(B)$
Step 3. Solve: $\tilde{z}=\left(\frac{2a}{\lambda_1}\Omega^{-1}+HM^{-1}H^T\right)^{-1}HM^{-1/2}b$
Step 4. Compute: $z=M^{-1/2}\tilde{z}$
Step 5. Compute: $x=M^{-1}b-M^{-1}H^Tz$
End

5. Experimental results

In this work, we compare our method with two state-of-the-art methods in dynamic MRI reconstruction, that are based on exploiting the transform domain sparsity and the rank-deficiency of the image sequence [12,13] and [14]. In [12,13], the sparsity penalty is the l_1-norm on the Spatio-temporal TV (total variation) and the rank-deficiency penalty is on the Schatten-q norm; this method is known as the k-t SLR. In [14] the sparsity penalty is the l_1-norm on the x-f space and the rank-deficiency is exploited via a power factorization based method which is similar to the Schatten-q norm.

All the methods require specification of the two parameters λ_1 and λ_2 – they control the relative importance of the sparsity and the low-rank penalties respectively. Unfortunately these parameters cannot be determined based on rigorous optimization theory. They need to be tuned. The tuning mechanisms for determining these values are not clearly mentioned in [12–14]. Therefore in this work, we follow a tuning methodology outlined in [9]. In the first step we determine the value of λ_1; to obtain λ_1 we put λ_2 to zero. Thus we only use the sparsity constraint. The value of λ_1 is determined by using the L-curve method [25] (after putting λ_2 to zero). Once the value of λ_1 is fixed, the value of λ_2 is then chosen by minimizing the error in the reconstruction, as compared with ground-truth. Effectively this means that the value of λ_2 has to be determined by manual tuning. For our algorithm, we also need to specify the value of ε; in this work it is assumed that the K-space data is not corrupted by noise hence ε is fixed at a small value of 10^{-3}.

Table 1
Reconstruction accuracy in NMSE.

Method →	k-t SLR [12,13]	[14]	Proposed analysis	Proposed synthesis
Dataset 1	0.13	0.12	0.09	0.08
Dataset 2	0.12	0.12	0.08	0.08

In [12,13] a value of $q=0.1$ is used for the Schatten-q norm. We use the same value of q for our proposed method. Our method also requires specifying the value of p in the l_p-norm; we use $p=0.1$. We carried out simple t-tests to determine the sensitivity of reconstruction accuracy to changes in value of p. We found that as long as p is between 0.1 and 0.3, the reconstruction accuracy does not significantly differ at 95% confidence level. But for higher values of p (0.5 and above) the reconstruction accuracy changes (deteriorates) significantly.

The Dynamic Contrast Enhanced (DCE) MRI data was collected from a 7 T Tesla Bruker MRI scanner at the University of British Columbia. Two datasets were acquired. The data was collected for studying subcutaneous tumor on the back of rats. The images are of size 128 × 64 pixels, and the time difference between acquisitions of two successive frames is 2.5 seconds. For each sequence, 1200 frames were acquired. The ground-truth images consisted of fully sampled K-space data. The same datasets were used for experiments on dynamic MRI reconstruction in [26].

For our experiments, partial K-space sampling was simulated by Variable Density randomly sampling, i.e., by omitting samples along the vertical direction. Experiments are carried out at an acceleration factor of 2 (50% sampling).

Results for quantitative evaluation are reported in Table 1. We report the Normalized Mean Squared Error ($NMSE=\|reconstructed-groundtruth\|_2/\|groundtruth\|_2$) for the whole dataset; i.e. the groundtruth signal consists of all the frames of the fully sampled K-space data and the reconstructed signal consists of all the frames reconstructed from partially sampled K-space data. As mentioned before, we compare our work with k-t SLR [12,13] and [14].

In order to test if the reconstruction error varies significantly we carried out t-tests. The pair-wise t-tests were carried out at 95% confidence level. The null hypothesis to be tested is: the reconstruction error between the compared pair of methods does not vary significantly. Results of the hypothesis testing are shown in Table 2.

From Table 2, it can be inferred that at 95% confidence level:

- The reconstruction error from k-t SLR [12,13] and [14] does not vary significantly.

Table 2
Results of t-test (h-values of pair-wise t-test).

Pair-wise tests →	k-t SLR & [14]	k-t SLR & proposed analysis	k-t SLR & proposed synthesis	Proposed analysis & [14]	Proposed synthesis & [14]	Proposed analysis & proposed synthesis
Dataset 1	1	0	0	0	0	1
Dataset 2	1	0	0	0	0	1

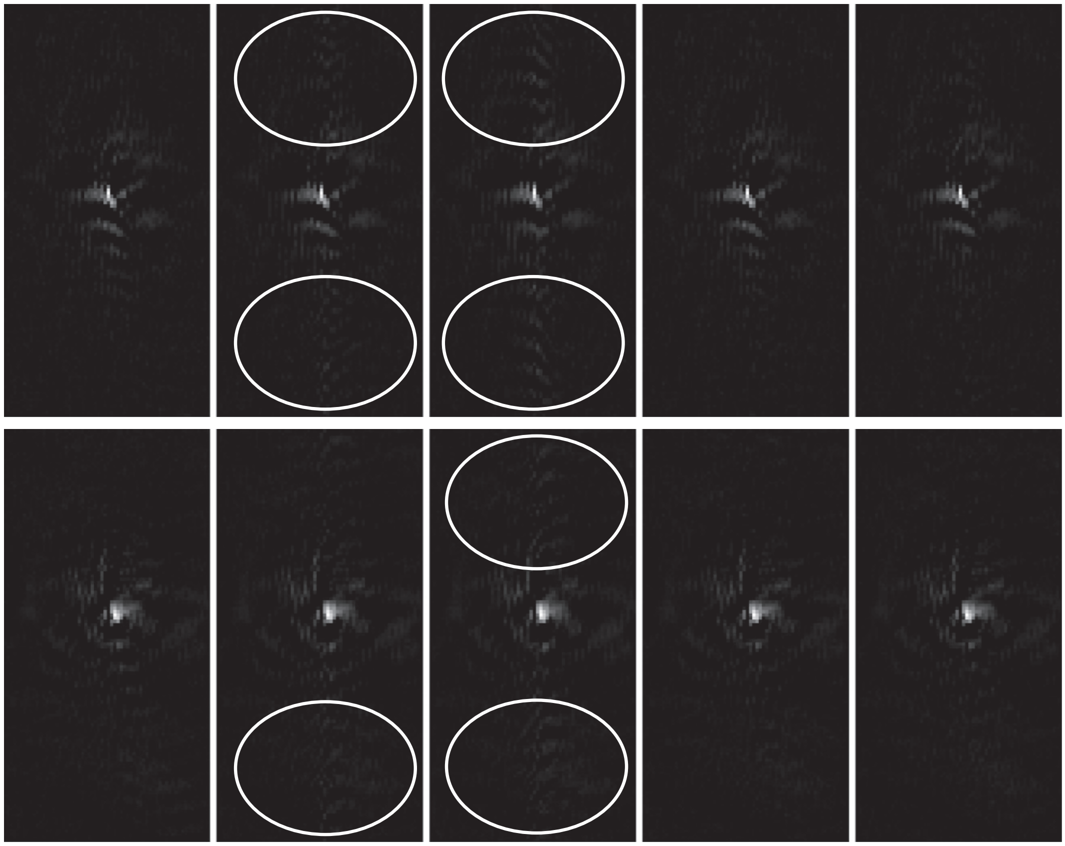

Fig. 1. Reconstructed Images. Left to Right – Groundtruth, k-t SLR [12,13] reconstruction, [14] reconstruction, proposed analysis prior, proposed synthesis prior.

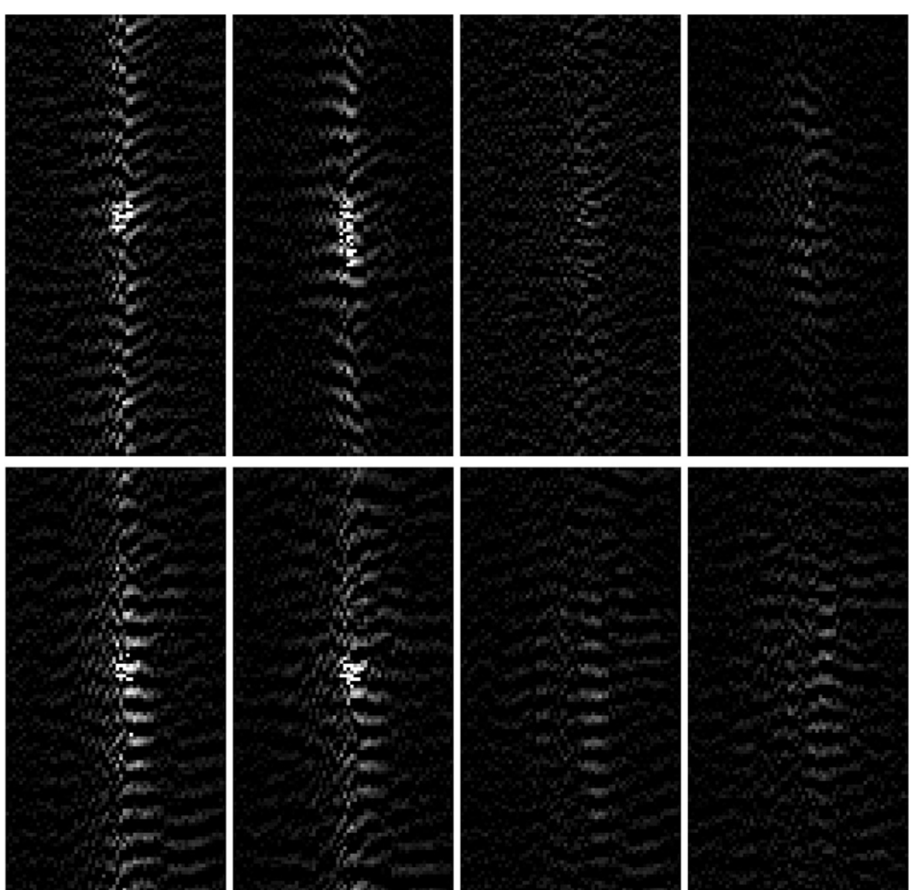

Fig. 2. Difference Images. Left to Right – k-t SLR [12,13] reconstruction, [14] reconstruction, proposed analysis prior, proposed synthesis prior.

• The k-t SLR [12,13] and the [14] yields significantly different (worse) reconstruction error compared to the proposed analysis and the synthesis prior methods.
• The reconstruction error from our proposed analysis and synthesis prior methods does not vary significantly.

Numerical results do not always provide the true nature of reconstruction. Therefore we provide qualitative reconstruction results from the experiments. For qualitative evaluation we randomly selected frame number 1096 from the dataset and frame number 283 from the second dataset. The reconstructed images and difference images (between groundtruth and reconstructed images) are shown in Figs. 1 and 2 respectively.

In Fig. 1 we have encircled the areas that show reconstruction artifacts. These are clearly visible in the reconstruction from the k-t SLR and the method proposed in [14]. Our proposed methods yield considerably better results; they do not show such distinct reconstruction artifacts. The superiority of our proposed methods can also be discerned from the difference images in Fig. 2. The difference images from k-t SLR and the method proposed in [14] show higher reconstruction error (brighter difference images) compared to ours (darker difference images). The qualitative results corroborate our inferences from quantitative analysis.

6. Conclusion

Recent techniques in dynamic MRI reconstruction (from under-sampled K-space data) [12–14] exploit the spatio-temporal correlation in the dynamic MRI sequence by posing the recovery problem as a least squares optimization with sparse (in a transform domain) and low-rank penalties. In [12,13] the sparsity is assumed to be in the spatio-temporal differencing domain and in [14] it is assumed to be in the *x-f* space.

Ideally the sparsity and low-rank penalties should be expressed in terms of the l_0-norm and the rank of matrix respectively. However both the l_0-norm and rank of matrix are NP hard penalties and thus are not feasible to be solved for practical problems. In the previous works [12–14] the l_0-norm is substituted by its convex surrogate the l_1-norm and the rank is substituted by its non-convex surrogate the Schatten-q norm ($0<q\leq 1$).

Previous studies in static MRI reconstruction [2,20,21] have showed that if non-convex sparsity penalty in the form of l_p-norm ($0<p\leq 1$) is used instead of the convex l_1-norm, better image reconstruction can be obtained. Following these studies we proposed to substitute the l_1-norm sparsity penalty in [12–14] by its non-convex counterpart – the l_p-norm. Thus our formulation for recovering the dynamic MRI sequence (from under-sampled K-space data) requires solving a least squares problem regularized by an l_p-norm and a Schatten-q norm. Depending on the sparsifying transform the l_p-norm can either be on a synthesis prior or on an analysis prior. Unfortunately there are no efficient algorithms to solve either the synthesis prior or the analysis prior problem. Thus in this work, we had to derive efficient algorithms to solve the said problems.

We carried out the experiments on two DCE MRI datasets that studied subcutaneous tumor on the back of rats. We compared our proposed methods with state-of-the-art techniques in dynamic MRI reconstruction that uses both sparsity and low-rank penalties for recovery [12–14]. Simple statistical analysis shows that our method is significantly better than existing ones. We also provide the reconstructed images for qualitative evaluation. It is clearly seen from the images that the aforementioned methods [12–14] show discernible reconstruction artifacts while our methods do not.

Acknowledgment

The author is thankful to Dr. Piotr Kozlowski and Henry S. Chen of the University of British Columbia, MRI Physics Lab for providing the experimental data.

References

[1] Lustig M, Donoho DL, Pauly JM. Sparse MRI: the application of compressed sensing for rapid MR imaging. Magn Reson Med 2007;58(6):1182-95.
[2] Trzasko J, Manduca A. Highly undersampled magnetic resonance image reconstruction via homotopic l0-minimization. IEEE Trans Med Imaging 2009;28(1):106-21.
[3] Gamper U, Boesiger P, Kozerke S. Compressed sensing in dynamic MRI. Magn Reson Med 2008;59(2):365-73.
[4] M. Lustig, J.M. Santos, D.L. Donoho, J.M Pauly "k-t SPARSE: High frame rate dynamic MRI exploiting spatio-temporal sparsity" ISMRM '06.
[5] Jung H, Ye JC, Kim EY. Improved k-t BLAST and k-t SENSE using FOCUSS. Phys Med Biol 2007;52:3201-26.
[6] Jung H, Park J, Yoo J, Ye JC. Radial k-t FOCUSS for high-resolution cardiac cine MRI. Magn Reson Med 2010;63:68-78.
[7] Jung H, Park J, Yoo J, Ye JC. k-t FOCUSS: a general compressed sensing framework for high resolution dynamic MRI. Magn Reson Med 2009;61:103-16.
[8] Chen L, Schabel MC, DiBella EVR. Reconstruction of dynamic contrast enhanced magnetic resonance imaging of the breast with temporal constraints. Magn Reson Imaging 2010;28(5):637-45.
[9] Adluru G, McGann C, Speier P, Kholmovski EG, Shaaban A, DiBella EVR. Acquisition and reconstruction of undersampled radial data for myocardial perfusion magnetic resonance imaging. J Magn Reson Imaging 2009;29:466-73.
[10] B. Zhao, J. P. Haldar, C. Brinegar, Z. P. Liang, "Low rank matrix recovery for real-time cardiac MRI", International Symposium on Biomedical, Imaging, pp. 996–999, 2010.
[11] J. P. Haldar, Z. P. Liang, "Low-Rank Approximations for Dynamic Imaging", International Symposium on Biomedical, Imaging, pp. 1052–1055, 2011.
[12] Lingala SG, Hu Y, DiBella EVR, Jacob M. Accelerated dynamic MRI exploiting sparsity and low-rank structure: k-t SLR. IEEE Trans Med Imaging 2011;30(5): 1042-54.
[13] S. G. Lingala, H. Yue, E. V. R. Dibella and M. Jacob, "Accelerated first pass cardiac perfusion MRI using improved k — t SLR" International Symposium on Biomedical, Imaging, pp. 1280–1283, 2011.
[14] B. Zhao, J. P. Haldar, A. G. Christodoulou, and Z. P. Liang, "Image reconstruction from highly undersampled (k, t)-space data with joint partial separability and sparsity constraints", IEEE Trans. Med. Imag., (accepted).
[15] Donoho D. Compressed sensing. IEEE Trans Inf Theory 2006;52(4):1289-306.
[16] Candès EJ, Romberg J, Tao T. Stable signal recovery from incomplete and inaccurate measurements. Commun Pure Appl Math 2006;59(8):1207-23.
[17] R. Saab, R. Chartrand, and Ö. Yilmaz, "Stable sparse approximation via nonconvex optimization", IEEE Int. Conf. on Acoustics, Speech, and, Signal Processing, pp. 3885–3888, 2008.
[18] Saab R, Yılmaz Ö. Sparse recovery by non-convex optimization – instance optimality. Appl Comput Harmonic Anal 2010;29(1):30-48.
[19] Chartrand R. Exact reconstruction of sparse signals via nonconvex minimization. IEEE Signal Process Lett 2007;14:707-10.
[20] A. Majumdar and R. K. Ward, "Under-determined Non-Cartesian MR Reconstruction", MICCAI, pp. 513-520, 2010.
[21] A. Majumdar and R. K. Ward, "On the choice of compressed sensing priors: an experimental study", signal processing: image communication (accepted).
[22] I. W. Selesnick and M. A. T. Figueiredo, "Signal restoration with overcomplete wavelet transforms: comparison of analysis and synthesis priors", Proceedings of SPIE, Vol. 7446 (Wavelets XIII), 2009.
[23] Choi S-CT, Paige CC, Saunders MA. MINRES-QLP: A Krylov subspace method for indefinite or singular symmetric systems. SIAM J Sci Comput 2011;33(4): 1810-36.
[24] Bai ZZ, Zhang SL. A regularized conjugate gradient method for symmetric positive definite system of linear equations. J Comput Math 2002;20:437-48.
[25] Hansen PC, O'Leary DP. The use of the L-curve in the regularization of discrete ill-posed problems. SIAM J Sci Stat Comput 1993;14:1487-503.
[26] Majumdar A. FOCUSS based Schatten-p norm minimization for real-time reconstruction of dynamic contrast enhanced MRI. IEEE Signal Process Lett 2012;9(5):315-8.